Disordered two-dimensional superconductors: Roles of temperature and interaction strength

Felipe Mondaini,[1] Thereza Paiva,[1] Raimundo R. dos Santos,[1] and R. T. Scalettar[2]
[1]*Instituto de Física, Universidade Federal do Rio de Janeiro, Caixa Postal 68528, 21941-972 Rio de Janeiro, RJ, Brazil*
[2]*Department of Physics, University of California, Davis, California 95616, USA*
(Received 23 July 2008; revised manuscript received 30 September 2008; published 19 November 2008)

We have considered the half-filled disordered attractive Hubbard model on a square lattice, in which the on-site attraction is switched off on a fraction f of sites, while keeping a finite U on the remaining ones. Through quantum Monte Carlo simulations for several values of f and U and for system sizes ranging from 8×8 to 16×16, we have calculated the configurational averages of the equal-time pair structure factor P_s and, for a more restricted set of variables, the helicity modulus ρ_s, as functions of temperature. Two finite-size scaling *Ansätze* for P_s have been used: one for zero temperature and the other for finite temperatures. We have found that the system sustains superconductivity in the ground state up to a critical impurity concentration f_c, which increases with U, at least up to $U=4$ (in units of the hopping energy). Also, the normalized zero-temperature gap as a function of f shows a maximum near $f\sim 0.07$ for $2\lesssim U\lesssim 6$. Analyses of the helicity modulus and of the pair structure factor led to the determination of the critical temperature as a function of f for $U=3$, 4, and 6: they also show maxima near $f\sim 0.07$, with the highest T_c increasing with U in this range. We argue that, overall, the observed behavior results from both the breakdown of charge-density-wave-superconductivity degeneracy and the fact that free sites tend to "push" electrons toward attractive sites; the latter effect being more drastic at weak couplings.

DOI: 10.1103/PhysRevB.78.174519 PACS number(s): 74.20.−z, 74.81.−g, 74.25.Dw, 74.78.−w

I. INTRODUCTION

The interplay between impurities and superconducting pairing has been a challenging problem for some time.[1] It has been argued[2] that as long as electronic states remain extended in the presence of weak disorder, superconductivity should not be affected; as disorder increases, however, superconductivity must eventually be suppressed. The consequences of this competition are especially interesting in two dimensions since the superconducting transition belongs to the xy-model universality class [the Kosterlitz-Thouless (KT) transition to a state without long-range order], while noninteracting electrons become localized in the presence of any amount of disorder. Indeed, by varying the thickness of thin films of Bi and Pb deposited on Ge substrates,[3] the sheet resistance $R_\square$ shows insulating behavior (i.e., it increases with decreasing temperature T) for the thinner samples and superconducting behavior for the thicker samples; the separatrix between these two regimes extrapolates to a quantum critical point as $T\to 0$ (Ref. 1) and one of the unresolved issues is whether or not R^*, the threshold value of $R_\square$, is universal, i.e., $R^*=R_Q\equiv h/4e^2$.

From the theoretical point of view, the two-dimensional behavior has been examined in a variety of ways. Some have exploited a bosonic description of Cooper pairs,[4,5] according to which electrons near the Fermi surface are paired and localization is driven by Coulomb repulsion among pairs. On the other hand, one may envisage a fermionic mechanism: Disorder enhances Coulomb repulsion among electrons, thus decreasing the effective screening (due to electron-phonon interactions in conventional superconductors) which in turn leads to the disappearance of Cooper pairs.[6] Intermediate pictures have also been proposed[7] within a phenomenological theory to address the issue of universality of R^*.

Since none of these approaches have succeeded in fully explaining experimental data, alternative routes should be sought. One possibility is to study simplified microscopic fermionic models in which disorder is incorporated in a fundamental and unbiased way. However, not much is known about models in which disorder is present in the pairing interaction. With the purpose of bridging this gap and due to the fact that disorder is more readily dealt with in real space, here we consider the disordered attractive Hubbard model, whose Hamiltonian reads,

$$H=-t\sum_{\langle \mathbf{r}\mathbf{r}'\rangle\sigma}(c^\dagger_{\mathbf{r}\sigma}c_{\mathbf{r}'\sigma}+\text{H.c.})-\mu\sum_{\mathbf{r}\sigma}n_{\mathbf{r}\sigma}-\sum_{\mathbf{r}}U(\mathbf{r})n_{\mathbf{r}\uparrow}n_{\mathbf{r}\downarrow}, \tag{1}$$

where $c^\dagger_{\mathbf{r}\sigma}(c_{\mathbf{r}\sigma})$ are fermion creation (destruction) operators at site $\mathbf{r}$ with spin σ, and $n_{\mathbf{r}\sigma}=c^\dagger_{\mathbf{r}\sigma}c_{\mathbf{r}\sigma}$ and H.c. stands for Hermitian conjugate of the previous term. The kinetic-energy lattice sum $\langle \mathbf{r}\mathbf{r}'\rangle$ is over nearest-neighbor sites on a two-dimensional square lattice and μ is the chemical potential; the hopping integral sets the energy scale, so we take $t=1$ throughout this paper. The on-site attraction $U(\mathbf{r})$ is chosen to take on the two values $U(\mathbf{r})=0$ and U with probabilities f and $1-f$, respectively; note that $U>0$ corresponds to attraction, according to our definition of the on-site term in Eq. (1). A review of the homogeneous model can be found in Ref. 8, while Ref. 9 deals with a recent extension of the model to describe nonrandom layered superconductors as the borocarbides.

The above model mimics the thin films of Bi and Pb being referred above, in the sense that the inverse film thickness tracks the concentration $1-f$ of attractive sites.[3] Additionally, it also describes the effects of negative-U centers, which are thought to be relevant to high-temperature superconductivity in the cuprates.[8,10] This model has been studied at mean-field level[11–13] and the main results, for a given electronic density, can be summarized as follows: (i) supercon-

ductivity in the ground state is destroyed for impurity concentrations above f_c; (ii) f_c decreases as U increases [very simple heuristic arguments[11] lead to $f_c=1-(U/W)^2$ in two dimensions, with $W=8t$ being the bandwidth]; and (iii) $T_c(f)/T_c(0)$ is a concave-down function of f, which vanishes at $f_c(U)$. Though mean-field approximations are useful as a first approach to the problem, one should be extremely cautious about their predictions for two-dimensional systems. For instance, for the pure system at half filling, the degeneracy of charge-density wave (CDW) and superconducting order leads to an effective three-component order parameter, thus suppressing the critical temperature to zero[14–16] by virtue of the Mermin-Wagner theorem;[17] mean-field approaches are unable to detect this feature and should therefore lead to unreliable results close to half filling. Indeed, recent quantum Monte Carlo (QMC) simulations have predicted that a small amount of disorder at half filling initially enhances superconductivity;[18] this was attributed to the impurity-induced breakdown of the above-mentioned degeneracy. In view of all this, a more thorough investigation of the model at half filling is clearly in order. Here we report on quantum Monte Carlo studies of the dependence of f_c with U as well as of the dependence of T_c with f, for different values of U; we recall that Ref. 18 was restricted to $U=4$ and $T=0$ only. As we will see, our predictions are very different from those of mean-field approaches.

The paper is organized as follows. In Sec. II we outline the QMC method and discuss the quantities used to locate the superconducting transitions. In Sec. III we present a finite-size scaling (FSS) analysis of data for superconducting correlations in the ground state, from which we extract the behavior of f_c with U. In Sec. IV we perform finite-temperature FSS analyses of data for superconducting correlations, as well as analyses of the superfluid density, to obtain $T_c(f)$ for different values of U. Finally, Sec. V summarizes our findings.

II. COMPUTATIONAL APPROACH

We use the determinant QMC method[19–23] to investigate the ground state as well as finite-temperature properties of the model. In this approach, the imaginary-time interval $(0;\beta)$ is discretized into M slices separated by the interval $\Delta\tau$ and a path-integral expression is written down for the partition function Z. The electron-electron interactions are decoupled by the introduction of a Hubbard-Stratonovich field.[20] The fermion degrees of freedom can then be integrated out analytically, leaving an expression for Z which involves an integral over the Hubbard-Stratonovich field with an integrand which is the product of two determinants of matrices whose dimensions equal the system size. We perform the integral stochastically. In the case of the attractive Hubbard model considered here, the traces over the spin-up and spin-down electrons are given by the determinant of the same matrix; the integrand is a perfect square and hence there is no sign problem.[21,23]

In order to study the physics at a particular lattice size $L\times L$ and value of f, we randomly choose fL^2 sites and set $U=0$ on those sites. We typically use 30–50 such realizations to average over the different disorder configurations. If fL^2 is not an integer, we average over the two adjacent integer values with appropriate weights. For each disorder configuration, observables are evaluated as the appropriate combinations of the Green's functions, which are given by matrix elements of the inverse of the matrix appearing as the integrand.[19,21–23] The average over different disorder configurations then yields the quantities of interest. Systematic errors in the calculated quantities associated with our choice of $\Delta\tau$ for the discretization of β are typically smaller than statistical errors, namely those arising from fluctuations for a single disorder realization as well as those arising from sample-to-sample variations.

As discussed previously,[18] a useful quantity to locate the transition is the configurationally averaged equal-time pairing structure factor,

$$P_s = \left[\sum_{\mathbf{r}} \Gamma(\mathbf{r})\right], \tag{2}$$

where $[\ldots]$ denotes average over disorder configurations (thus restoring translational invariance), and the pairing correlation function is

$$\Gamma(\mathbf{r}) \equiv \langle \Delta(\mathbf{i})\Delta^{\dagger}(\mathbf{i}+\mathbf{r}) + \text{H.c.}\rangle, \tag{3}$$

where $\langle\ldots\rangle$ denotes ensemble average with

$$\Delta(\mathbf{r}) = c_{\mathbf{r}\downarrow}c_{\mathbf{r}\uparrow}. \tag{4}$$

The different scaling behaviors of P_s, in the ground state and at finite temperatures, will be discussed in Secs. III and IV.

Further, current-current correlations probe the superfluid weight and provide an alternative way to detect the destruction of superconductivity.[24] We define

$$\Lambda_{xx}(\mathbf{r},\tau) = \langle j_x(\mathbf{r},\tau)j_x(0,0)\rangle, \tag{5}$$

where

$$j_x(\mathbf{r},\tau) = e^{H\tau}\left[it\sum_{\sigma}(c^{\dagger}_{\mathbf{r}+\hat{x},\sigma}c_{\mathbf{r},\sigma} - c^{\dagger}_{\mathbf{r},\sigma}c_{\mathbf{r}+\hat{x},\sigma})\right]e^{-H\tau}, \tag{6}$$

and the Fourier transform in space and imaginary time,

$$\Lambda_{xx}(\mathbf{q},\omega_n) = \frac{1}{N_s}\sum_{\mathbf{r}}\int_0^{\beta} d\tau e^{i\mathbf{q}\cdot\mathbf{r}}e^{-i\omega_n\tau}\Lambda_{xx}(\mathbf{r},\tau), \tag{7}$$

where N_s is the number of lattice sites, and $\omega_n=2n\pi/\beta$.

The longitudinal part of the current-current correlation function satisfies the f-sum rule, which relates its value to the kinetic energy K_x,

$$\Lambda^{\mathrm{L}} \equiv \lim_{q_x\to 0}\Lambda_{xx}(q_x,\ q_y=0,\ \omega_n=0) \tag{8}$$

$$\Lambda^{\mathrm{L}} = K_x, \tag{9}$$

where $K_x=\langle -t\Sigma_{\sigma}(c^{\dagger}_{\mathbf{r}+\hat{x},\sigma}c_{\mathbf{r},\sigma}+c^{\dagger}_{\mathbf{r},\sigma}c_{\mathbf{r}+\hat{x},\sigma})\rangle$. Meanwhile, in the superconducting state the transverse part,

$$\Lambda^{\mathrm{T}} \equiv \lim_{q_y\to 0}\Lambda_{xx}(q_x=0,\ q_y,\ \omega_n=0), \tag{10}$$

can differ from the longitudinal part, the difference being the superfluid stiffness D_s,

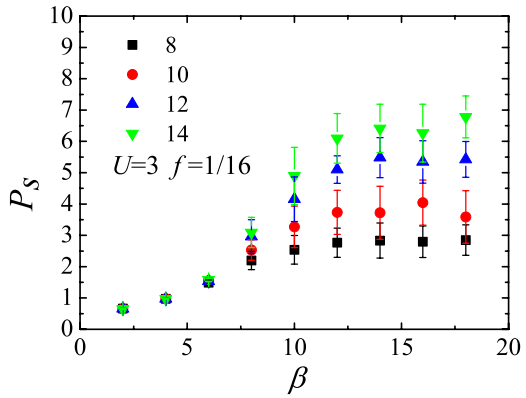

FIG. 1. (Color online) Configurationally averaged equal-time pair structure factor P_s as a function of the inverse temperature β, for different lattice sizes at half filling and concentration of free sites $f=1/16$.

$$D_s/\pi = [\Lambda^{\mathrm{L}} - \Lambda^{\mathrm{T}}] = [K_x - \Lambda^{\mathrm{T}}]. \tag{11}$$

Thus the current-current correlations provide an alternative complementary method to the equal-time pair correlations for looking at the superconducting transition.

III. GROUND-STATE PROPERTIES: $f_c(U)$

As remarked above, there is no "sign problem" for the attractive Hubbard model, so we can do computations at very low temperatures (large β), as shown in Fig. 1 for the data of unscaled P_s. We recall that throughout this paper we only consider the case of a half-filled band. The error bars result from the dispersion in the average values taken over disorder configurations.

The finite-size scaling behavior of P_s allows us to extract quantitative information about the superconducting transition. As shown by Huse,[25] the spin-wave correction to the pair structure factor in the ground state is expected to be inversely proportional to the linear lattice size,

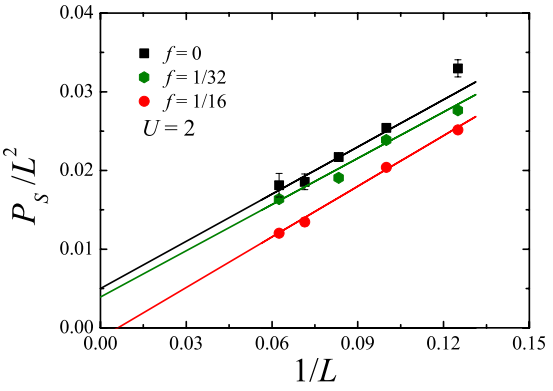

FIG. 2. (Color online) Zero-temperature scaling of the configurationally averaged equal-time pair structure factor, for $U=2$, and for different disorder concentrations f. For each f, the intersection with the vertical axis yields the (squared) zero-temperature gap; see Eq. (12).

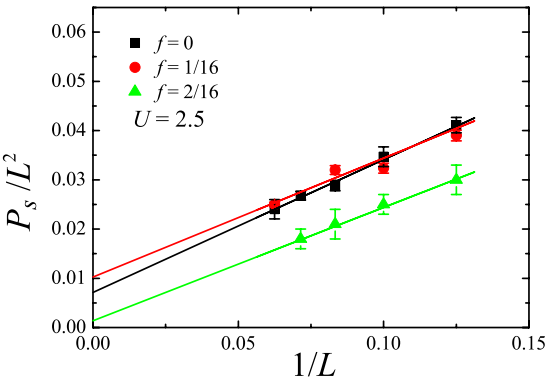

FIG. 3. (Color online) Same as Fig. 2, but for $U=2.5$.

$$\frac{P_s}{L^2} = |\Delta_0|^2 + \frac{a}{L}, \tag{12}$$

where Δ_0 is the superconducting gap function at zero temperature, and $a \equiv a(U,f)$ is independent of L.

In Figs. 2–5 we plot the $T \to 0$ extrapolated values of P_s/L^2 versus $1/L$, for linear lattice sizes ranging from $L=8$ to 16, and $U=2$, 2.5, 3, and 6 (data for $U=4$ can be found in Fig. 4 of Ref. 18). According to Eq. (12), each intercept with the vertical axis provides an estimate for Δ_0^2 (the square of the zero-temperature gap) for the values of U and f considered. For the pure system ($f=0$), Δ_0 is plotted as a function of U in Fig. 6: the observed increase of Δ_0 (at least up to $U \sim 6$) is due to an increase in the average site double occupancy. Indeed, Fig. 7 shows the double occupancy on attractive sites $d_A \equiv \langle n_\uparrow n_\downarrow - 1/4 \rangle$ as a function of U for both the pure system and for several disordered configurations. The overall behavior is an increase in d_A with U and, for a fixed U, this double occupancy increases with f, as it can be seen from its strong-coupling limit,

$$\langle n_\uparrow n_\downarrow - 1/4 \rangle = \frac{1}{4}\frac{1+f}{1-f}, \quad U \to \infty. \tag{13}$$

In order to compare the effects of disorder for different attraction intensities, for each U we normalize the zero-temperature gap Δ by their respective pure system values Δ_0; the result is displayed in Fig. 8. For $2.5 \lesssim U < 6$, the normal-

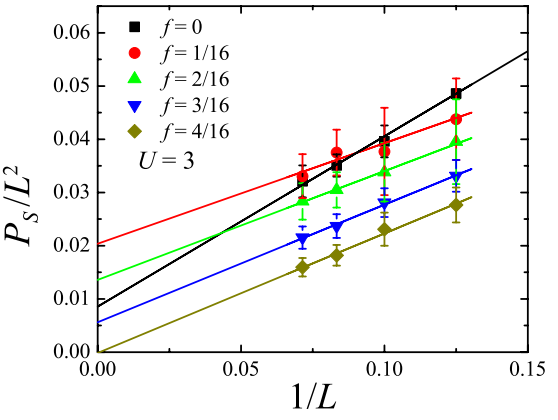

FIG. 4. (Color online) Same as Fig. 2, but for $U=3$.

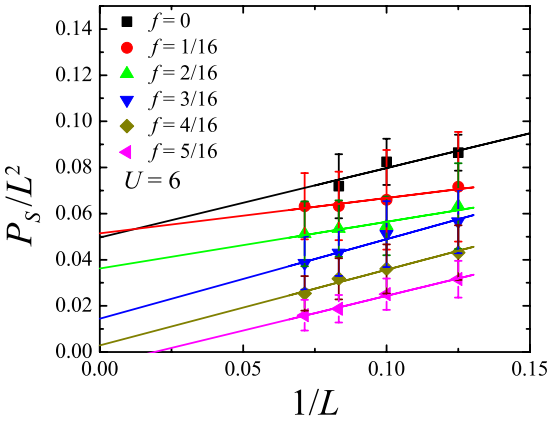

FIG. 5. (Color online) Same as Fig. 2, but for $U=6$.

ized gaps initially increase with disorder, reaching maxima $[\Delta/\Delta_0]_{\max}$ around $f\sim 0.07$. It should be noticed that $[\Delta/\Delta_0]_{\max}$, in turn, does not behave monotonically as a function of U but displays a maximum for $U=3$ among the values of U examined. Another crucial information extracted from Fig. 8 is that a maximum of Δ/Δ_0 is absent for $U=6$. This different behavior for larger U therefore indicates that the disorder-induced breakdown of CDW-superconductivity degeneracy is not the only mechanism at play: for smaller U, the presence of free sites contributes to a decrease in the single occupancy by "pushing" electrons to the attractive sites. For larger U, the pairs are so tightly bound that the relative weight of single occupancy is smaller and disorder has hardly any effect in forcing the electrons to occupy the attractive sites. Figure 7 indeed shows that the percentual enhancement in double occupancy due to disorder is larger for $U\sim 4$ than for $U\sim 6$. As disorder increases, the presence of free sites strongly disturbs pair coherence and the gap decreases. The initial increase with disorder has also been predicted for anisotropic superconductors with mesoscopic phase separation.[26,27]

We can obtain the dependence of f_c with U by extrapolating the data for Δ/Δ_0 to zero. The intercept with the horizontal axis of each of the curves in Fig. 8 provides f_c for the corresponding U and the result is displayed in Fig. 9; the

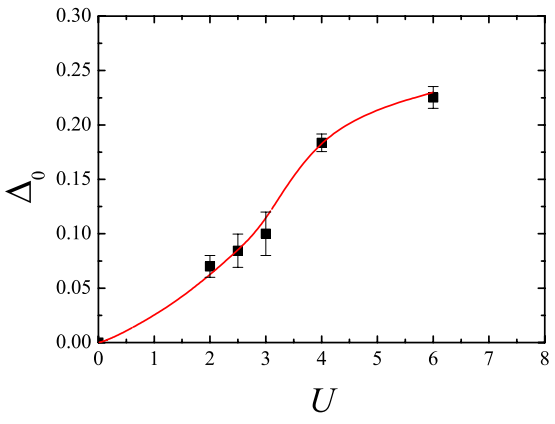

FIG. 6. (Color online) Zero-temperature gap for the pure system, obtained from the $f=0$ data, together with Eq. (12). The full line is a guide to the eye.

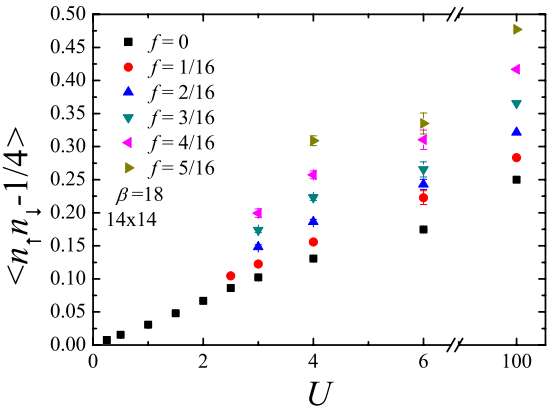

FIG. 7. (Color online) Average double occupancy on attractive sites as a function of U, for the pure case and for several disordered configurations. Data are for 14×14 lattices and for $\beta=18$. Data for $U=100$ correspond to the strong-coupling limit [Eq. (13)].

error bars reflect the uncertainties in the extrapolations of Δ/Δ_0 to zero in Fig. 8. It should be noted that f_c initially (i.e., for $U\lesssim 2$) increases very slowly with U, which should be attributed to the fact that the pairs are not so strongly bound for small U, so that a small amount of free sites destroys phase coherence. As U increases, the pairs become more tightly bound and a larger amount of disorder can be sustained before the free sites switch their roles from pushing electrons onto attractive sites to that of destroying phase coherence.

This behavior is in disagreement with mean-field predictions, according to which f_c should decrease with U,[11] though for $U\gtrsim 4$, f_c appears to be decreasing with U and the agreement with the mean-field approach would set in. In some situations, Bogoliubov-de Gennes-type theories do a good job of capturing spatial charge redistribution driven by disorder; a recent comparison between mean-field and exact approaches in systems with diagonal disorder indicates that although charge redistribution may be well described within mean-field approaches, local spin correlations are not.[28] In the case considered here, however, this discrepancy can be attributed—to some extent—to two intertwined mechanisms. First, there is the fact that a three-component order parameter

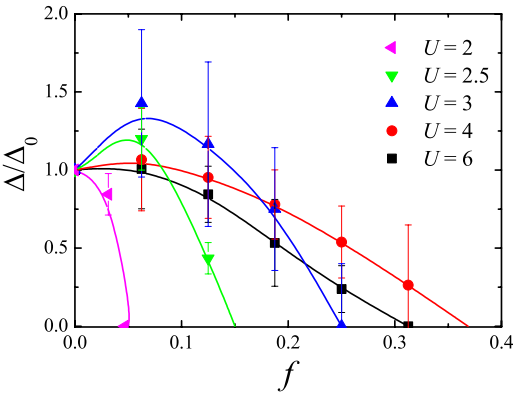

FIG. 8. (Color online) Normalized zero-temperature gaps as functions of impurity concentration, for different values of U. Full lines are guides to the eye.

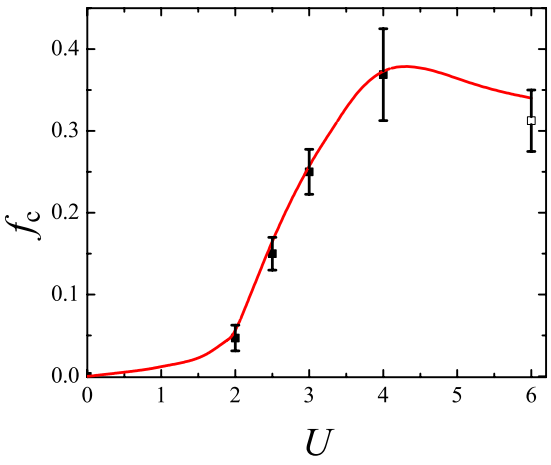

FIG. 9. (Color online) Critical impurity concentration as a function of U, obtained from Fig. 8. The full line is a guide to the eye.

(CDW+superconducting) is split by the disorder into a one-component (CDW) and a two-component (superconducting) order parameters and they fluctuate independently; the present situation is even more sensitive due to the nature of the Kosterlitz-Thouless transition itself. Second, in the present case disorder affects the pairing interaction, so that the charge redistribution may not be adequately described, i.e., to the point that the above-mentioned switching of roles played by the free sites cannot be picked up if fluctuations are not included in a fundamental way.

It is also worth noting that the strong-coupling pure attractive Hubbard model (at half filling) can be mapped onto an isotropic Heisenberg model.[29,30] Therefore, the fact that f_c displays such strong dependence with U is a clear indication that the mechanisms of superconductivity suppression by impurities are very different from those occurring in diluted magnetic insulators, which are driven by classical percolation.[31] That is, if one is interested in singling out the geometrical aspects of impure superconductors, a model of correlated dilution should be more appropriate.

IV. FINITE-TEMPERATURE PROPERTIES: $T_c(f,U)$

Another consequence of the two-component nature of the order parameter is that at finite temperatures the superconducting-normal phase transition for the pure system belongs to the Kosterlitz-Thouless universality class. As such, for $0<T\leq T_c$, one expects that asymptotically,

$$\Gamma(r) \sim r^{-\eta(T)}, \tag{14}$$

where $\Gamma(r)$ is defined by Eq. (3), and $\eta(T)$ increases monotonically between $\eta(0)=0$ and $\eta(T_c)=1/4$.[32,33] The finite-size scaling behavior of P_s is therefore obtained upon integration of $\Gamma(r)$ over a two-dimensional system of linear dimension L. One then has[15]

$$P_s = L^{2-\eta(T_c)}F(L/\xi), \quad L \gg 1, \quad T \to T_c^+, \tag{15}$$

where $F(z)$ is a finite-size scaling function of the variable $z \equiv L/\xi$, with

$$\xi \sim \exp\left[\frac{A}{(T-T_c)^{1/2}}\right], \tag{16}$$

where A is a constant; in the thermodynamic limit, one recovers $P_s \sim \xi^{7/4}$. As discussed in Ref. 16, we can obtain estimates of T_c by plotting $L^{-7/4}P_s(L,\beta)$ as functions of β, for different L, and by looking for intersections or merges of curves for consecutive values of L. This procedure was supported by independent estimates of the critical temperature through calculations of the superfluid stiffness D_s and using the universal jump at T_c; see Ref. 16 for details.

The general aspects of the universality class of the superconducting transition should remain valid in the presence of disorder, since one still deals with a two-component order parameter. Further, numerical evidence has been gathered for the xy model[34] showing that $\eta(T_c)=1/4$ even in the presence of disorder; this is in agreement with the Harris criterion, which essentially states that disorder is irrelevant (in the renormalization-group sense) if the specific-heat exponent α is positive.[35] In view of this, our data analyses for the finite-temperature transitions can follow along the same lines as those for the pure system,[16] with both P_s and D_s now being understood as the configurationally averaged equal-time pair-correlation function and superfluid stiffness, respectively.

Let us first consider the helicity modulus (HM),[24] which is given by

$$\rho_s = \frac{D_s}{4\pi e^2}, \tag{17}$$

where D_s is defined in Eq. (11), and we take $e=1$ in our units. At the KT transition, the following universal-jump relation involving the helicity modulus holds:[36]

$$T_c = \frac{\pi}{2}\rho_s^-, \tag{18}$$

where ρ_s^- is the value of the helicity modulus just below the critical temperature. Thus, on universality grounds we may assume the same holds for a configurationally averaged ρ_s and we can obtain T_c by plotting $\rho_s(T)$ and by looking for the intercept with $2T/\pi$. Figure 10 shows data for $U=4$ and we see that the intercepts occur at $T_c=0.125\pm0.015$, 0.12 ± 0.01, 0.105 ± 0.008, and 0.080 ± 0.015 for $f=1/16$, 2/16, 3/16, and 4/16, respectively. Similarly to the pure case,[16] we have found that the estimates for T_c thus obtained are not too sensitive to the lattice sizes used. These estimates appear as empty circles in Fig. 11.

In Fig. 12 we show the scaled configurationally averaged equal-time pair structure factor as a function of the inverse temperature β, for $U=4$ and different system sizes, for a given concentration of disorder. For usual second-order phase transitions, similar curves for two successive linear lattice sizes should cross at a single point, thus leading to estimates for critical inverse temperatures. For KT transitions, on the other hand, curves for different (but sufficiently large) lattice sizes should merge above a certain β_c.[37] In the present case, we estimate β_c as the smallest value for which the curves for the smallest size superimpose—within error bars—with the one for the largest size; this ensures that the

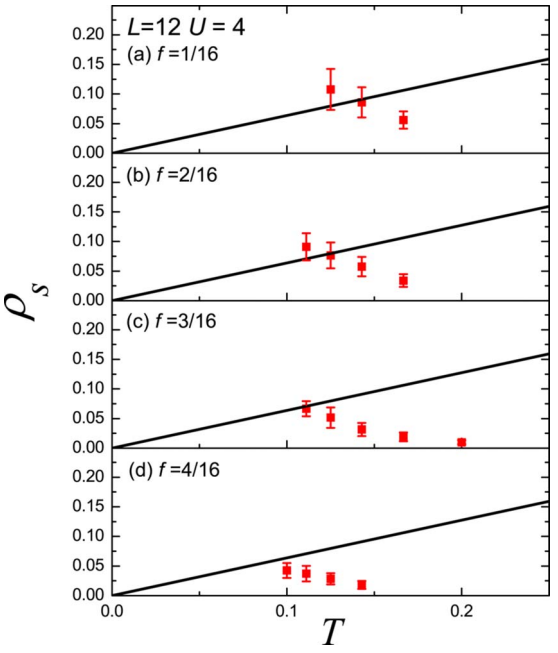

FIG. 10. (Color online) Configurationally averaged helicity modulus as a function of temperature, for $U=4$ and different impurity concentrations f, for a 12×12 lattice. In each panel, the straight line corresponds to $2T/\pi$.

error bars for data corresponding to intermediate sizes will also superimpose. Thus, applying this criterion to the data in Fig. 12 yields $\beta_c=8\pm1$; this procedure is systematically repeated for other values of f, and we obtain the $T_c(f)$ data for $U=4$ shown in Fig. 11. The estimates thus obtained are in excellent agreement with those obtained from the HM, thus adding credence to our merging criterion.

Given the fact that the calculations of configurationally averaged helicity moduli are very consuming in terms of computer time (for a given disorder configuration the CPU time is increased significantly due to the τ integration and one performs averages over typically 50 disorder configurations), for other values of U we only use data for P_s to estimate $T_c(U,f)$. From Figs. 13 and 14 (which yield $\beta_c=12\pm1$ and $\beta_c=6\pm1$, respectively), as well as from similar ones for other values of f, we obtain the estimates for $T_c(f)$ for $U=3$ and 6 shown in Fig. 11.

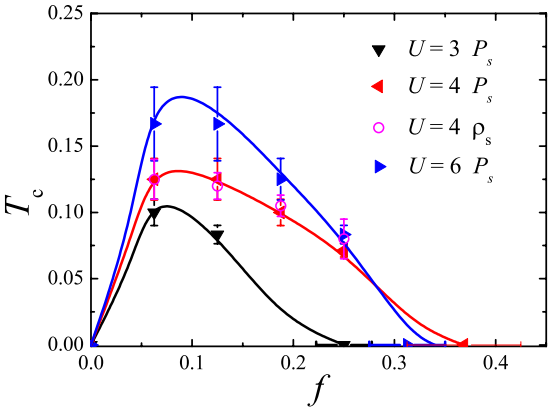

FIG. 11. (Color online) Critical temperature (in units of the bandwidth) for superconductivity, as a function of impurity concentration, f, for different values of the on-site attraction U. Full symbols have been obtained through the scaling of the pairing structure factor (P_s), whereas the empty circles correspond to data obtained through the helicity modulus (ρ_s). Full lines are guides to the eye.

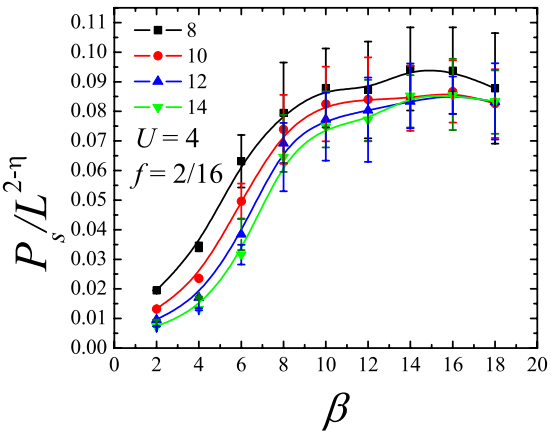

FIG. 12. (Color online) Scaled configurationally averaged equal-time pair structure factor as a function of the inverse temperature β, for different lattice sizes ($L\times L$) at half filling, concentration of free sites $f=2/16$, and $U=4$. The curves are labeled by the linear lattice size L and full lines are guides to the eye.

Several interesting physical features emerge from Fig. 11. First, $T_c(0)=0$ as a result of the CDW-superconductivity degeneracy at half filling; however, any finite amount of disorder breaks this degeneracy and T_c rises. Second, in all curves, T_c displays a maximum at some $f_{\max}$, as a result of the interplay between the above-mentioned degeneracy and the behavior of the smallest energy scale Δ. Third, we expect $T_c\to0$ at $f_c(U)$; since above f_c, superconductivity cannot be sustained even in the ground state. Finally, near f_c, T_c displays the convex shape observed in experiments;[3] the steepness of the decrease in $T_c(f)$ can therefore be used to fit an effective U by experimental data. As a final comment, one should have in mind that some of these results should change drastically as the system is doped away from half filling. Indeed, since in this case CDW-superconductivity degeneracy is already broken in the pure system, T_c should display

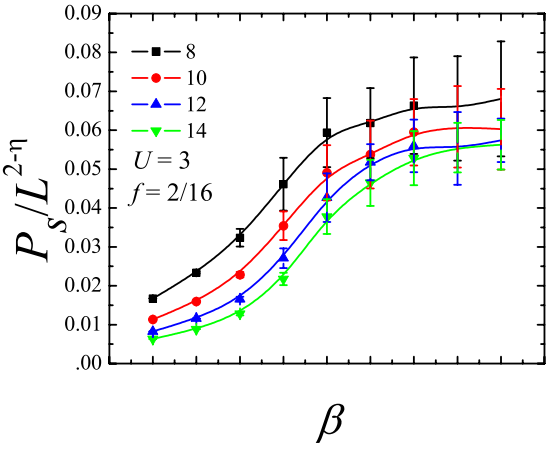

FIG. 13. (Color online) Same as Fig. 12, but for $U=3$.

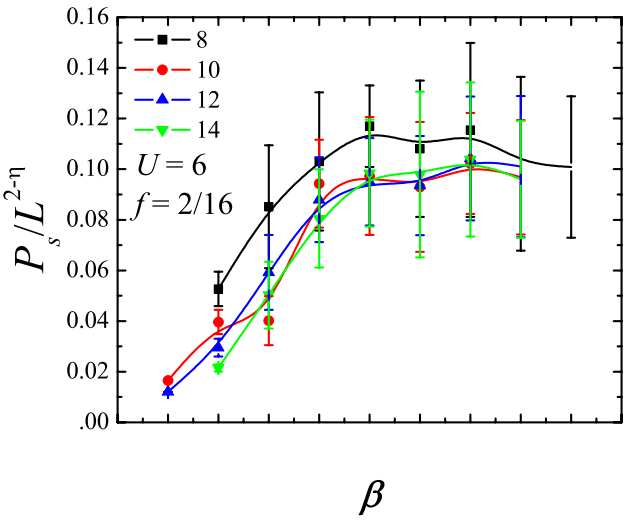

FIG. 14. (Color online) Same as Fig. 12, but for $U=6$.

a monotonic decrease with f for a given U; nonetheless, we can still expect T_c to be a convex function of f.

V. CONCLUSIONS

We have addressed the issue of disorder in two-dimensional superconductors. To this end, we have considered a simple model, namely, the attractive Hubbard model, in which the on-site attraction is switched off on a fraction f of sites, while keeping a finite U on the remaining ones; the model is defined in such a way that $U>0$ in the attractive case [see Eq. (1)]. Through quantum Monte Carlo simulations for typically 50 disorder configurations, we have calculated the configurational averages of the equal-time pair structure factor and, for $U=4$, the helicity modulus as functions of temperature; there is no minus-sign problem in the attractive case. The continuous $O(2)$ symmetry of the superconducting order parameter allows us to use a spin-wavelike finite-size scaling form for the ground-state behavior, from which the zero-temperature gap was calculated; at finite temperatures, the usual finite-size scaling form for the Kosterlitz-Thouless transition was used to calculate the critical temperature, which was checked for consistency against data for the helicity modulus. Our numerical data are consistent with the following findings: (i) Superconductivity in the ground state is destroyed above an impurity concentration f_c; (ii) At least up to $U=4$, this critical concentration increases with increasing U, slowly for $U\lesssim 2.5$, and then fast up to $U\sim 4$; this behavior does not agree with mean-field predictions due to the important role played by fluctuations, not included in the latter approach. The error bars prevent us from ascertaining that f_c decreases with U above $U=4$, but it may be that the mean-field behavior is recovered in this regime, since fluctuations should become less important for large U. At any rate, the transition at zero temperature is not driven by purely geometrical aspects, such as in dilute insulating magnets. (iii) In the range between $U=2.5$ and $U\lesssim 6$, the normalized zero-temperature gap initially (i.e., small disorder) increases with disorder, as a result of both the breakdown of CDW-superconductivity degeneracy and the fact that free sites "push" the electrons toward attractive sites and (iv) near the critical concentration of defects beyond its maximum value, T_c is a convex function of f, as observed in experiments.

Overall, we conclude that the random attractive Hubbard model is a promising working ground to investigate the interplay between impurities and pairing. By tuning two variables at half filling, namely, the impurity concentration and the pairing potential, we have found instances in which small disorder either hardly affects superconductivity or enhances it. It should therefore be of interest to check whether these features remain valid away from half filling. Further, the present model can be used, with suitable changes, to investigate other disordered BCS superconductors, such as three-dimensional carbon-substituted MgB_2 (Ref. 38) and MgB_2/MgO superstructures.[39]

ACKNOWLEDGMENTS

This work was supported by the Brazilian Agencies CNPq, CAPES, FAPERJ, Instituto de Nanotecnologia/MCT, and Fundação Universitária José Bonifácio/UFRJ, by the DOE under Grant No. DE-FG01-06NA26204 and by the NSF under Grant No. OISE 0803230. The authors are grateful to the *E-Infrastructure Shared Between Europe and Latin America* (EELA) project for the use of their computational facilities.

[1] A. M. Goldman and N. Marković, Phys. Today **51**(11), 39 (1998).
[2] P. W. Anderson, J. Phys. Chem. Solids **11**, 26 (1959).
[3] D. B. Haviland, Y. Liu, and A. M. Goldman, Phys. Rev. Lett. **62**, 2180 (1989).
[4] M. P. A. Fisher, P. B. Weichman, G. Grinstein, and D. S. Fisher, Phys. Rev. B **40**, 546 (1989).
[5] M. P. A. Fisher, G. Grinstein, and S. M. Girvin, Phys. Rev. Lett. **64**, 587 (1990).
[6] A. I. Larkin, Ann. Phys. **8**, 785 (1999).
[7] M. V. Feigel'man, A. I. Larkin, and M. A. Skvortsov, Phys. Rev. Lett. **86**, 1869 (2001).
[8] R. Micnas, J. Ranninger, and S. Robaszkiewicz, Rev. Mod. Phys. **62**, 113 (1990).
[9] T. Paiva, M. El-Massalami, and R. R. dos Santos, J. Phys.: Condens. Matter **15**, 7917 (2003).
[10] J. A. Wilson, J. Phys.: Condens. Matter **13**, R945 (2001).
[11] G. Litak and B. L. Györffy, Phys. Rev. B **62**, 6629 (2000).
[12] K. Aryanpour, E. R. Dagotto, M. Mayr, T. Paiva, W. E. Pickett, and R. T. Scalettar, Phys. Rev. B **73**, 104518 (2006).
[13] K. Aryanpour, T. Paiva, W. E. Pickett, and R. T. Scalettar, Phys. Rev. B **76**, 184521 (2007).

[14] R. T. Scalettar, E. Y. Loh, J. E. Gubernatis, A. Moreo, S. R. White, D. J. Scalapino, R. L. Sugar, and E. Dagotto, Phys. Rev. Lett. **62**, 1407 (1989).
[15] A. Moreo and D. J. Scalapino, Phys. Rev. Lett. **66**, 946 (1991).
[16] T. Paiva, R. R. dos Santos, R. T. Scalettar, and P. J. H. Denteneer, Phys. Rev. B **69**, 184501 (2004).
[17] N. D. Mermin and H. Wagner, Phys. Rev. Lett. **17**, 1133 (1966).
[18] D. Hurt, E. Odabashian, W. Pickett, R. Scalettar, F. Mondaini, T. Paiva, and R. R. dos Santos, Phys. Rev. B **72**, 144513 (2005).
[19] R. Blankenbecler, D. J. Scalapino, and R. L. Sugar, Phys. Rev. D **24**, 2278 (1981).
[20] J. E. Hirsch, Phys. Rev. B **28**, 4059 (1983).
[21] J. E. Hirsch, Phys. Rev. B **31**, 4403 (1985).
[22] S. R. White, D. J. Scalapino, R. L. Sugar, E. Y. Loh, J. E. Gubernatis, and R. T. Scalettar, Phys. Rev. B **40**, 506 (1989).
[23] R. R. dos Santos, Braz. J. Phys. **33**, 36 (2003).
[24] D. J. Scalapino, S. R. White, and S. Zhang, Phys. Rev. B **47**, 7995 (1993).
[25] D. A. Huse, Phys. Rev. B **37**, 2380 (1988).
[26] A. J. Coleman, E. P. Yukalov, and V. I. Yukalova, Physica C **243**, 76 (1995).
[27] V. I. Yukalov and E. P. Yukalova, Phys. Rev. B **70**, 224516 (2004).
[28] X. Chen, A. Farhoodfar, T. McIntosh, R. J. Gooding, and P. W. Leung, J. Phys.: Condens. Matter **20**, 345211 (2008).
[29] V. J. Emery, Phys. Rev. B **14**, 2989 (1976).
[30] R. R. dos Santos, Phys. Rev. B **48**, 3976 (1993).
[31] R. B. Stinchcombe, in *Phase Transitions and Critical Phenomena*, edited by C. Domb and J. L. Lebowitz (Academic, New York, 1983), Vol. 7.
[32] J. M. Kosterlitz and D. J. Thouless, J. Phys. C **6**, 1181 (1973).
[33] B. Berche, A. I. F. Sanchez, and R. Paredes, Europhys. Lett. **60**, 539 (2002).
[34] B. Berche, A. I. Farinas-Sanchez, Y. Holovatch, and R. Paredes, Eur. Phys. J. B **36**, 91 (2003).
[35] A. B. Harris, J. Phys. C **7**, 1671 (1974).
[36] D. R. Nelson and J. M. Kosterlitz, Phys. Rev. Lett. **39**, 1201 (1977).
[37] M. N. Barber, in *Phase Transitions and Critical Phenomena*, edited by C. Domb and J. L. Lebowitz (Academic, New York, 1983), Vol. 8.
[38] S. M. Kazakov, R. Puzniak, K. Rogacki, A. V. Mironov, N. D. Zhigadlo, J. Jun, C. Soltmann, B. Batlogg, and J. Karpinski, Phys. Rev. B **71**, 024533 (2005).
[39] W. Siemons, M. A. Steiner, G. Koster, D. H. A. Blank, M. R. Beasley, and A. Kapitulnik, Phys. Rev. B **77**, 174506 (2008).